The American Journal of Pathology, Vol. 186, No. 12, December 2016

ELSEVIER

The American Journal of PATHOLOGY

ajp.amjpathol.org

BIOMARKERS, GENOMICS, PROTEOMICS, AND GENE REGULATION

Ornithine Decarboxylase Is Sufficient for Prostate Tumorigenesis via Androgen Receptor Signaling

Amita Shukla-Dave,*† Mireia Castillo-Martin,‡§ Ming Chen,¶ Jose Lobo,† Nataliya Gladoun,‡ Ana Collazo-Lorduy,‡‖ Faisal M. Khan,‡ Vladimir Ponomarev,† Zhengzi Yi,** Weijia Zhang,** Pier P. Pandolfi,¶ Hedvig Hricak,† and Carlos Cordon-Cardo‡

From the Departments of Medical Physics and Radiology,† Memorial Sloan Kettering Cancer Center, New York, New York; the Departments of Pathology‡ and Medicine,** Icahn School of Medicine at Mount Sinai, New York, New York; the Department of Pathology,§ Champalimaud Centre for the Unknown, Lisbon, Portugal; the Beth Israel Deaconess Medical Center,¶ Harvard Medical School, Boston, Massachusetts; and the Spanish Society of Medical Oncology,‖ Madrid, Spain*

Accepted for publication August 9, 2016.

Address correspondence to Carlos Cordon-Cardo, M.D., Ph.D., Department of Pathology, Icahn School of Medicine at Mount Sinai, 1 Gustave L. Levy Pl, New York, NY 10029. E-mail: carlos.cordon-cardo@mssm.edu.

Increased polyamine synthesis is known to play an important role in prostate cancer. We aimed to explore its functional significance in prostate tumor initiation and its link to androgen receptor (AR) signaling. For this purpose, we generated a new cell line derived from normal epithelial prostate cells (RWPE-1) with overexpression of ornithine decarboxylase (ODC) and used it for *in vitro* and *in vivo* experiments. We then comprehensively analyzed the expression of the main metabolic enzymes of the polyamine pathway and spermine abundance in 120 well-characterized cases of human prostate cancer and high-grade prostate intraepithelial neoplasia (HGPIN). Herein, we show that the ODC-overexpressing prostate cells underwent malignant transformation, revealing that ODC is sufficient for de novo tumor initiation in 94% of injected mice. This oncogenic capacity was acquired through alteration of critical signaling networks, including *AR*, *EIF2*, and *mTOR/MAPK*. RNA silencing experiments revealed the link between AR signaling and polyamine metabolism. Human prostate cancers consistently demonstrated up-regulation of the main polyamine enzymes analyzed (ODC, polyamine oxidase, and spermine synthase) and reduction of spermine. This phenotype was also dominant in HGPIN, rendering it a new biomarker of malignant transformation. In summary, we report that ODC plays a key role in prostate tumorigenesis and that the polyamine pathway is altered as early as HGPIN. *(Am J Pathol 2016, 186: 3131—3145; http://dx.doi.org/10.1016/j.ajpath.2016.08.021)*

The polyamine pathway has been reported to play an essential role in cell growth and mitochondrial functions.[1—4] The ornithine decarboxylase (ODC) enzyme, encoded by the *ODC1* gene, has been identified as the critical rate-limiting enzyme in this metabolic pathway.[5,6] It has been previously reported that *ODC* is a transcriptional target of the androgen receptor (AR),[7] with its potential oncogenic properties being ascribed to the pleiotropic effects of AR-responsive biology in prostate cancer, including aberrant metabolic activities.

In a previous report describing ODC overexpression in prostate cancer, the number of prostate cancer cases examined was limited compared to the numbers of normal prostate and benign prostatic hyperplasia tissue samples assessed.[6] Normal prostatic glands have high levels of polyamines, mainly spermine, whereas in tumor tissue, spermine levels are reduced.[8] Studies by our group and others using noninvasive proton magnetic resonance spectroscopy have shown that the level of polyamines is higher than the choline level significantly more often in benign prostate tissue than in prostate cancer.[9—12]

The chain of molecular events involved in tumor initiation [ie, the transformation of normal epithelium to high-

Supported by the Margaret Dorrance Strawbridge Foundation, NIH/National Cancer Institute Cancer Center Support grant P30 CA008748 (Department of Radiology, Memorial Sloan Kettering Cancer Center), NIH grant R01-CA-076423 (A.S.-D. and H.H.), and NIH grant P01-CA-087497 (C.C.C. and M.C.-M.).

A.S.-D. and M.C.-M. contributed equally to this work.

Disclosures: None declared.

http://dx.doi.org/10.1016/j.ajpath.2016.08.021

grade prostate intraepithelial neoplasia (HGPIN) and to invasive cancer] has been difficult to analyze in the entire prostate gland because of the multifocal nature and heterogeneity of prostate tumors.[13] Several candidate genes and pathways have been implicated in prostate cancer development and progression, including *PTEN*, *p27/KIP1*, and *Nkx3.1* tumor suppressor genes, as well as the oncogenes c-*myc* and *Bcl-2*.[14–16] Gene fusions involving *TMPRSS2* and several *ETS* family members have been found in a high percentage of prostate cancers, and it has been suggested that they may play an important role in prostate tumorigenesis.[17] These gene fusions have been found in at least 16% of HGPIN lesions, and all of the HGPIN lesions with these gene fusions were associated with cancer that shared the same fusion pattern; however, 60% of *TMPRSS2-ERG* fusion prostate cancers had associated fusion-negative HGPIN.[18] Recently, genomic alterations observed in prostate cancer genomes were found to be direct descendants of HGPIN, although more genetic changes are required for progression.[19] Hence, there is a critical need to explore the implications of polyamines in prostate tumor initiation and to reveal the mechanisms by which the main enzymes elicit their tumorigenic effects.

Given the importance of *ODC* in prostate cancer, we generated a new normal prostate cell line overexpressing ODC to mechanistically elucidate, for the first time, *ODC*'s potential oncogenic role. This study is also the first to comprehensively analyze the expression of the main metabolic enzymes and abundance of the critical amine of the polyamine pathway in a large and well-annotated cohort of patients with prostate cancer, including cases of HGPIN.

Materials and Methods

Cell Culture

The RWPE1 cell line was purchased from ATCC (Manassas, VA) and maintained in RPMI 1640 medium with 20% fetal bovine serum, according to manufacturer's protocols, at 37°C in a humidified air atmosphere at 5% CO_2. RWPE1 cells were generated by immortalization with HPV16 in 1997 by Bello et al[20] and characterized as nontumorigenic and noninvasive. The metastatic prostate cancer cells CWR22, LNCaP, and VCaP were purchased from ATCC and maintained in RPMI 1640 medium and Dulbecco's modified Eagle's medium with 10% fetal bovine serum at 37°C in a humidified air atmosphere at 5% CO_2.

Gene Silencing and Transient and Stable Transfection and Infection

We generated a stable cell line (named RWPE1_ODC) overexpressing ODC. *ODC* cDNA [catalog number MHS1011-7509233 Human MGC-verified FL Cdna (IRAU) clone ID: 5088190; Thermo Fisher Scientific, Lafayette, CO] was cloned into a SFG-CBR IRES green fluorescent protein vector (courtesy of Dr. Vladimir Ponomarev) (Figure 1A), as previously described.[21] The 293-GPG cells (courtesy of Dr. Vladimir Ponomarev, Memorial Sloan Kettering Cancer Center, New York, NY) were used as a retroviral packaging system and were transfected using x-tremeGENE 9 DNA Transfection Reagent (Roche, Indianapolis, IN). The newly generated cells were then sorted for green fluorescent protein, and overexpression of ODC in the stable RWPE1_ODC cell line at the mRNA level was assessed by quantitative RT-PCR (RT-qPCR) (Figure 1B), and at the protein level by immunoblot and immunofluorescence (Figure 1, C and D).

To address the functional link between *ODC* and *AR*, we transiently infected the prostate cancer cells LNCaP and VCaP with two independent siRNA duplexes targeted to human *ODC-1* (SASI_Hs01_00223603 and SASI_Hs01_00223604; Sigma-Aldrich, St. Louis, MO), and one with siGenome nontarget siRNA (D-001210-02-20; GE Dharmacon, Lafayette, CO). A total of 1×10^5 cells were seeded in 6-well plates and cultured in media with 10% charcoal-stripped fetal bovine serum for 48 hours. Transfections were then performed using Lipofectamine RNAiMAX (Invitrogen, Life Technologies, Grand Island, NY) with 50 nmol/L of indicated siRNA in Opti-MEM reduced serum media. Cells were recovered into media with charcoal-stripped fetal bovine serum at 12 hours after transfection. At 48 hours after transfection, cells were treated with 10 nmol/L dihydrotestosterone (Sigma-Aldrich), followed by RT-qPCR after 6 hours of treatment and immunoblotting after 24 hours of treatment.

RNA Extraction

RNA was extracted from cell lines using the RNeasy Mini Kit and QIAshredder (Qiagen, Valencia, CA), following the manufacturer's protocol, to perform both RT-qPCR and gene expression analyses.

RT-qPCR

First, strand cDNA was synthesized using Oligo dT and the SuperScript III First-Strand Synthesis System (Invitrogen, Carlsbad, CA), following the manufacturer's instructions. RT-qPCR was performed on a Mastercycler epgradient S realplex (Eppendorf, Enfield, CT) in accordance with the manufacturer's instructions. In a final volume of 20 μL, the RT-qPCR contained 10 μL of 2× QuantiTect SYBR Green PCR Master Mix (Qiagen, Valencia, CA), 1 μL of cDNA, and 2 μL of the primers. The primers used are summarized in Table 1. The thermal cycling conditions included the following: initial denaturation at 95°C for 15 minutes, followed by 40 cycles of denaturation at 94°C for 30 seconds, annealing at 60°C for 40 seconds, and elongation at 72°C for 30 seconds. The PCR products were analyzed by melting curve analysis to confirm that no by-products were formed. The relative concentrations of the PCR products derived

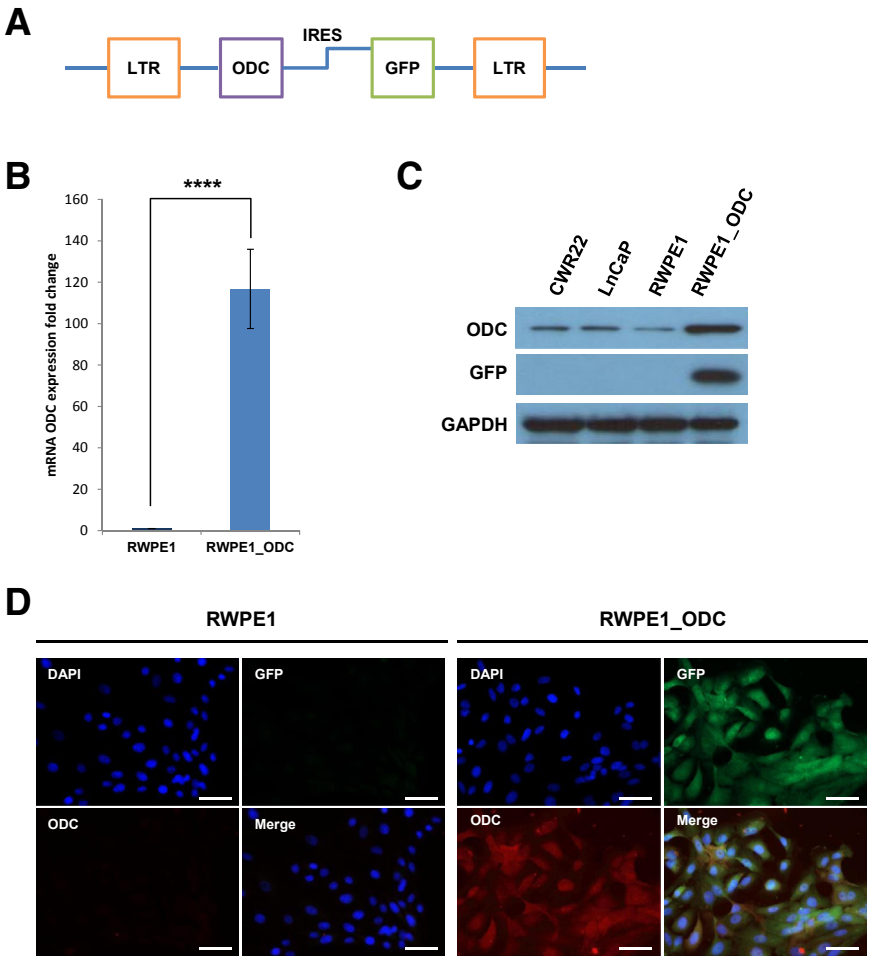

Figure 1 Generation and validation of a stable cell line overexpressing ornithine decarboxylase (ODC). **A:** Schematic representation of the construct generated to overexpress *ODC* in RWPE-1 cells. **B:** Quantification of three independent experiments of the relative fold increase of *ODC* mRNA levels in the RWPE1_ODC compared to the parental cells (*t*-test). **C:** Representative immunoblot of ODC and green fluorescent protein (GFP) in RWPE1 and RWPE1_ODC compared to prostate cancer cell lines CWR22 and LnCaP. **D:** Representative immunofluorescence analysis of ODC and GFP. RWPE1, parental cell line; RWPE1_ODC, stable cell line overexpressing ODC. $n = 3$ for each cell line for experiment (**B**). $^{****}P < 0.0001$. Scale bars = 100 μm (**D**). GAPDH, glyceraldehyde-3-phosphate dehydrogenase; IRES, internal ribosome entry site; LTR, long terminal repeats.

from the target gene were calculated using realplex software version 2.0 (Eppendorf) and the ΔΔCT method. All samples were run in triplicate and were normalized against actin ($n = 3$ in each of the three experiments performed).

Gene Expression Analyses

Whole-genome gene expression profiling was performed by the Genomics CORE using the HumanHT-12 Expression BeadChip (Illumina Inc., San Diego, CA), following manufacturer's instructions, in RWPE1_P and RWPE1_ODC ($n = 3$ for each cell line). The bioinformatics analyses were performed using the Bioconductor package version 3.4 (Roswell Park Cancer Institute, Buffalo, NY), TIGR Multiple Experiment Viewer software version 4.0,[22] and Significance Analysis of Microarrays software version 4.0 (Standford University, Stanford, CA). Genes differentially expressed were assessed by the DAVID Bioinformatics Resources for enrichment analysis of gene ontology categories. Gene ontology categories enriched on the highest hierarchical level (level 5 or higher) at statistical significance ($P < 0.01$) were taken into consideration. Pathway analyses were performed using the Ingenuity System. Data are publicly available through the Gene Expression Omnibus repository (*http://www.ncbi.nlm.nih.gov/geo*; accession number GSE82179).

Immunoblot Analysis

For immunoblotting, cells were lysed in radioimmunoprecipitation assay lysis buffer (Boston BioProducts, Ashland, MA), including protease inhibitor cocktail (Roche). Proteins were resolved by 4% to 20% SDS-PAGE and transferred to a nitrocellulose membrane. Blots were blocked with 5% nonfat dry milk and probed with primary antibodies as follows: green fluorescent protein (rabbit polyclonal; Abcam, Cambridge, MA), β-actin (mouse monoclonal, clone AC-15; Sigma-Aldrich), p44/42 mitogen-activated protein kinase (MAPK; rabbit monoclonal, clone 137F5; Cell Signaling Technology, Danvers, MA), phospho-p44/42 MAPK (Thr202/Tyr204, rabbit monoclonal, clone 20G11; Cell Signaling Technology), mammalian target of rapamycin (mTOR; rabbit monoclonal, clone 7C10; Cell Signaling Technology), phospho-mTOR (Ser2448, rabbit polyclonal; Cell Signaling Technology), p70S6 kinase (rabbit polyclonal; Cell Signaling Technology), phospho-4E-BP1 (Thr37/46, rabbit

Table 1 List of Primers Used for RT-qPCR

Gene	Primer	Sequence
ODC	Forward	5′-ACGTTCAATGGCTTCCAGAG-3′
	Reverse	5′-ATTGCTGCATGAGTTGCCACGCA-3′
	Probe	5′-ATGTGATGTCAGGGCCTGC-3′
PSA	Forward	5′-ACGCTGGACAGGGGGCAAAAG-3′
	Reverse	5′-GGGCAGGGCACATGGTTCACT-3′
TMPRSS2	Forward	5′-CAGGAGTGTACGGGAATGTGATGGT-3′
	Reverse	5′-GATTAGCCGTCTGCCCTCATTTGT-3′
FKBP5	Forward	5′-TCTCATGTCTCCCCAGTTCC-3′
	Reverse	5′-TTCTGGCTTTCACGTCTGTG-3′
AR	Forward	5′-CAGTGGATGGGCTGAAAAAT-3′
	Reverse	5′-GGAGCTTGGTGAGCTGGTAG-3′
ERG	Forward	5′-CACGAACGAGCGCAGAGTTAT-3′
	Reverse	5′-CTGTACTCCATAGCGTAGGATCT-3′
RPLP0	Forward	5′-GCTTCCTGGAGGGTGTCC-3′
	Reverse	5′-GGACTCGTTTGTACCCGTTG-3′

RT-qPCR, quantitative RT-PCR.

monoclonal, clone 236B4; Cell Signaling Technology), erythroblast transformation-specific–related gene (rabbit monoclonal, clone EPR3864; Abcam), AR (N-20, rabbit polyclonal; Santa Cruz Biotechnology Inc., Dallas, TX), prostate-specific antigen (PSA; K92110R; Meridian Life Science, Memphis, TN), as well as the same antibodies against ODC, polyamine oxidase (PAO), spermine synthase (SPSY), and spermine used for immunofluorescence (see below). Horseradish peroxidase–conjugated anti-rabbit and anti-mouse secondary antibodies (GE Healthcare Life Sciences, Piscataway, NJ) were used. Reactive bands were visualized using electrochemiluminescence plus Western blotting detection reagents (GE Healthcare Life Sciences).

DFMO Treatment

Cells were treated with D,L-α-difluoromethylornithine (DFMO; Santa Cruz Biotechnology Inc.) at 100 μmol/L (suspended in distilled sterile water) for up to 72 hours to inhibit ODC activity, as previously described.[23] Proliferation assays were performed as described below with cells in regular medium and cells with DFMO.

Putrescine Treatment

RWPE-1 cells were treated with putrescine (Sigma-Aldrich) at 100 μmol/L (suspended in distilled water), as previously described.[24] Proliferation and invasion assays were performed as explained below with RWPE-1 cells in regular medium and medium with putrescine.

Cell Proliferation Assay

A total of 2×10^3 cells were seeded in a 96-well plate. Cell viability was determined at 24, 48, 72, 96, 120, and 144 hours by using the CellTiter 96 Aqueous One Solution Cell Proliferation Assay kit (Promega, Madison, WI), according to the manufacturer's protocol. Absorbance was measured at 490 and 655 nm (used as a background reading) in a Synergy H1 Hybrid multimode microplate reader (Biotek, Winooski, VT). Data are presented as the mean value of three separate experiments for sixtuplicate wells ($n = 6$ for each time point for cell line in each of the three experiments).

Cell Cycle Analysis

For both cell lines, 1×10^6 cells were seeded in a 10-cm plate and allowed to grow for 24 hours. Cells were then harvested, pelleted, and fixed with 70% ethanol for 12 hours and washed with 1× phosphate-buffered saline. Cells were stained with propidium iodide solution at 5% in Triton–phosphate-buffered saline for 20 minutes at room temperature, and analyzed in a BD LSRII flow cytometer (BD Biosciences, San Jose, CA). Cell cycle phases were analyzed with the FlowJo software version 9.9.4 (TreeStar, Ashland, OR) in three independent experiments ($n = 3$ for each cell line in each of the three experiments).

In Vitro Invasion Assay

In vitro invasion assays were performed using BD BioCoat Matrigel Invasion Chambers (8-μm pore; BD Biosciences, San Jose, CA) in 24-well tissue culture plates, according to manufacturer's protocol. Cells were placed in serum-free media 24 hours before invasion assay set-up. Then, 5×10^5 cells were seeded per well and allowed to invade toward the underside of the chamber for 48 hours at 37°C. After incubation, Calcein AM solution (BD Biosciences) was added, and fluorescence of invaded cells was read at a wavelength of 494 to 517 nm (excitation/emission) on a SpectraMax M5e Multimode microplate reader (Molecular Devices, Sunnyvale, CA). Membranes were then stained with DAPI, and cell invasion was assessed using a Fluorescent Nikon Eclipse 50i microscope (Morrell Instruments Co., Inc., Melville, NY). Experiments were performed three times in duplicates ($n = 6$ for each time point for cell line in each of the three experiments).

Mouse Experiments

All assays were performed on 5- to 6-week-old male nonobese diabetic severe combined immunodeficiency γ mice purchased from Jackson Laboratories (Bar Harbor, ME). Animal use and care followed institutional guidelines established by Icahn School of Medicine at Mount Sinai and its Institutional Animal Care and Use Committee. For the tumor xenograft experiments, 1×10^6 RWPE1_P and RWPE1_ODC cells were injected in nonobese diabetic severe combined immunodeficiency γ mice. Three independent experiments were performed, including eight mice for each arm (parental and ODC-overexpressing cells) and mice were injected twice, in the right and left flanks ($n = 16$ for each cell line in each of the three experiments). Tumors

were allowed to develop for up to 6 months or whenever they reached a size of 1 cm^3. If a tumor developed in one flank to the size limit, we surgically removed it and let the mouse be alive up to 6 months. Tumors were measured twice every week with a caliper, and histologically analyzed after sacrificing the mice after 6 months, using cell injection, resection, and fixation with 10% formalin.

Study Design for Human Samples

A sample size calculation was performed for the differential expression of four biomarkers (three enzymes and spermine) across the two groups (normal and diseased). A minimum desired fold difference of 1.5 at a power level of 0.9 (rather than the traditional 0.8) was used, as a robust result for the biomarker was desired. Varying degrees of SD were modeled up to a maximum of 1.5, suggesting a sample size range of 35 to 78 samples in each group. A total of 128 prostate cancer patients who underwent radical prostatectomy between January 1991 and December 2004 and who had not received any adjuvant therapy were included in the study. The protocol was approved by the institutional review board and was compliant with the Health Insurance Portability and Accountability Act. Follow-up clinical information was available from 120 (93.75%) patients (Table 2). The primary outcome measure was the time (in months) to biochemical recurrence [defined as two consecutive detectable increasing PSA levels (>0.2 ng/mL) 4 weeks or more after surgery] or specific mortality after surgery.

Tissue Microarrays of Prostate Samples and Patient Cohort

Four tissue microarrays were built following institutional review board–approved protocol. Sections from formalin-fixed, paraffin-embedded prostatectomy specimens were stained with hematoxylin and eosin and reviewed to identify viable, morphologically representative areas of normal prostate glands and acinar adenocarcinoma from which needle core samples could be taken. From each specimen, triplicate tissue cores with diameters of 0.6 mm were punched and arrayed onto a recipient paraffin block using a precision instrument (Beecher Instruments Inc., Sun Prairie, WI). Sections (5 μm thick) of these tissue microarray blocks were stained with hematoxylin and eosin and used for immunofluorescence analysis. These tissue microarrays included acinar prostate adenocarcinoma ($n = 120$), and matched normal prostate glands ($n = 103$) as well as additional matched HGPIN ($n = 18$).

Immunofluorescence Analysis

Immunofluorescence analysis was performed blindly by an experienced uropathologist (M.C.-M.) on sections from these four tissue microarrays following standard staining procedure. Briefly, sections (5 μm thick) were deparaffinized and then submitted to antigen retrieval by steamer treatment for 15 minutes in 10 mmol/L citrate buffer at pH 6.0. Subsequently, sections were incubated in 10% normal donkey serum for 30 minutes, followed by primary antibody incubation overnight at 4°C. Then, slides were incubated with fluorescent-labeled anti-rabbit and anti-mouse immunoglobulins at a 1:200 dilution for 30 minutes (Invitrogen). DAPI was used as nuclear counterstain. Primary antibodies to detect critical enzymes and amines of the polyamine pathway included ODC (mouse monoclonal, clone ODC-29; Abcam), SPSY (rabbit polyclonal; Santa Cruz Biotechnology Inc.), PAO (mouse monoclonal, clone

Table 2 Patient Clinicopathological Characteristics ($n = 120$)

Characteristics	Value
Age at diagnosis, years*	60.8 (40–74)
Preoperative PSA, ng/mL*	11.3 (0.9–118.0)
Preoperative PSA, risk stratification†‡	
<10 ng/mL	75 (65.2)
10–20 ng/mL	26 (22.6)
>20 ng/mL	14 (12.2)
Preoperative PSA, dichotomous†‡	
<20 ng/mL	101 (87.8)
≥20 ng/mL	14 (12.2)
Surgical Gleason score†	
5	7 (5.9)
6	28 (23.3)
7	58 (48.3)
8	21 (17.5)
9	6 (5.0)
Surgical Gleason score, risk stratification†	
≤6	35 (29.2)
7	58 (48.3)
≥8	27 (22.5)
Surgical Gleason score, dichotomous†	
≤7	93 (77.5)
>7	27 (22.5)
Pathological stage†	
pT2	53 (44.2)
pT3	62 (51.6)
pT4	5 (4.2)
Pathological stage, risk stratification†	
≤pT2a	4 (3.3)
pT2b-pT2c	49 (40.9)
≥pT3	67 (55.8)
Pathological stage, dichotomous†	
Organ confined	53 (44.2)
Non–organ confined	67 (55.8)
BCR†§	48 (45.7)
BCR time, months*§	62.0 (3.0–187.0)
OS time, months*¶	103.6 (3.0–222.0)

*Data are given as mean (range).
†Data are given as number (percentage).
‡Data from five patients were missing.
§BCR data were available in 105 patients.
¶OS data were available in 117 patients.
BCR, biochemical recurrence; OS, overall survival; PSA, prostate-specific antigen.

C-3; Santa Cruz Biotechnology Inc.), and spermine (rabbit polyclonal; Abcam). To confirm the sensitivity and specificity of antibodies, positive and negative controls were run in parallel on paraffin-embedded tissue sections. ODC expression was characterized by a fine granular cytoplasmic staining, whereas PAO, SPSY, and spermine showed a diffuse cytoplasmic distribution. The immunoreactivity for each antibody was scored considering the percentage of cells displaying a positive immunostaining profile [from undetectable (0%) to homogeneous expression (100%)]. Average values of the representative cores from each arrayed sample were obtained, and a positive cutoff for statistical analyses was determined at 10% protein expression, which is commonly used as a standard cutoff for immunohistochemical analyses. Slides were analyzed with a Fluorescent Nikon Eclipse 50i microscope (Nikon Instruments, Melville, NY) equipped with a SPOT Insight2MP Mosaic camera and SPOT Advanced software version 5.0 (Diagnostic Instruments, Sterling Heights, MI).

Statistical Analysis

Statistical analyses were performed with SPSS version 19.0 (SPSS Inc., Chicago, IL). For the *in vitro* analyses, data were displayed as a mean value of three different experiments, and *t*-test was used to assess significance. Genes significantly dysregulated in RWPE1_ODC cells in comparison to RWPE1 parental lines were identified by using the Limma test $P < 0.05$ and greater than twofold change. To analyze the associations between protein expression values and clinicopathological variables, we used a *t*-test when one variable was continuous and the other qualitative and a χ^2 test or Fisher exact test when both variables were qualitative. The associations of molecular and clinicopathological variables with biochemical recurrence-free survival and overall survival were assessed using the log-rank test. Survival curves were plotted using standard Kaplan-Meier method. A two-sided value of $P < 0.05$ was considered statistically significant.

Results

Overexpression of *ODC* Is Sufficient for Malignant Transformation of Prostate Epithelial Cells

We first analyzed the polyamine pathway in two commercially available metastatic prostate cancer cell lines (CWR22 and LNCap) and the immortalized normal epithelial prostate cell line (RWPE1). Levels of the polyamine enzymes ODC, PAO, and SPSY were higher in the two cancer cell lines than in the normal counterpart, whereas spermine abundance showed the opposite trend (Figure 2A). Because of the critical relevance of ODC, we centered our study on this enzyme to further elucidate its potential role in prostatic tumor initiation and progression. Using RWPE1 cells, we generated a stable cell line overexpressing ODC, which we termed RWPE1_ODC. On stable transfection, RWPE1_ODC cells displayed high levels of ODC compared to their parental counterpart, both at the mRNA level (>100-fold increase) (Figure 1B) and the protein level (>20-fold increase) (Figure 1, C and D).

Proliferative activity was assessed by MTS [3-(4,5-dimethylthiazol-2-yl)-5-(3-carboxymethoxyphenyl)-2-(4-sulfophenyl)-2H-tetrazolium)] assay, and, as expected, RWPE1_ODC cells showed a significantly higher proliferative index than the parental line ($P < 0.01$) (Figure 2B). However, as would be expected of diploid populations, parental and RWPE1_ODC cells showed no significant differences on flow cytometry analysis (data not shown). After performing Matrigel invasion assays, we observed that the ODC-overexpressing cells displayed a significantly higher invasive ability (Figure 2C), thus confirming that RWPE1_ODC cells had malignant features.

To determine whether ODC was the critical factor involved in the malignant phenotype, we treated RWPE1_P and RWPE1_ODC cells with a well-known ODC inhibitor (DFMO). This experiment confirmed that the increase in proliferation was because of ODC overexpression, since treated RWPE1_ODC cells showed a significant decrease in proliferation (Figure 2D), whereas the effect in parental cells was much lower. Furthermore, we observed that these malignant features could be phenocopied by putrescine addition, since RWPE1_P cells treated with 100 μmol/L of putrescine showed a significant increase in cell proliferation (Figure 2E) as well as in Matrigel invasion (Figure 2F). This malignant phenotype was subsequently tested by s.c. injecting 1×10^6 cells in 24 nonobese diabetic severe combined immunodeficiency γ mice and monitoring them over a 6-month period. As previously described by the group that generated this normal prostate line, RWPE1 cells were nontumorigenic,[20] whereas tumor was palpated in 94% (45/48) of mice after injection with RWPE1_ODC cells (Figure 2G). The mean time to palpation was 48.0 days (range, 29.0 to 81.0 days). Histological analyses revealed that tumors corresponded to high-grade carcinomas and were morphologically characterized by increased mitotic activity and prominent nuclear atypia, including the presence of macronucleoli (Figure 2H). Taken together, these observations validate the hypothesis that the polyamine metabolic pathway is significantly involved in prostate tumorigenesis, and that ODC overexpression is sufficient for tumor initiation.

ODC Malignant Transformation Is Linked to Specific Genetic Alterations

To further characterize the altered genetic pathways after ODC overexpression, we performed gene expression analyses of RWPE1_ODC and parental RWPE1 cells. These studies revealed 113 up-regulated and 234 down-regulated

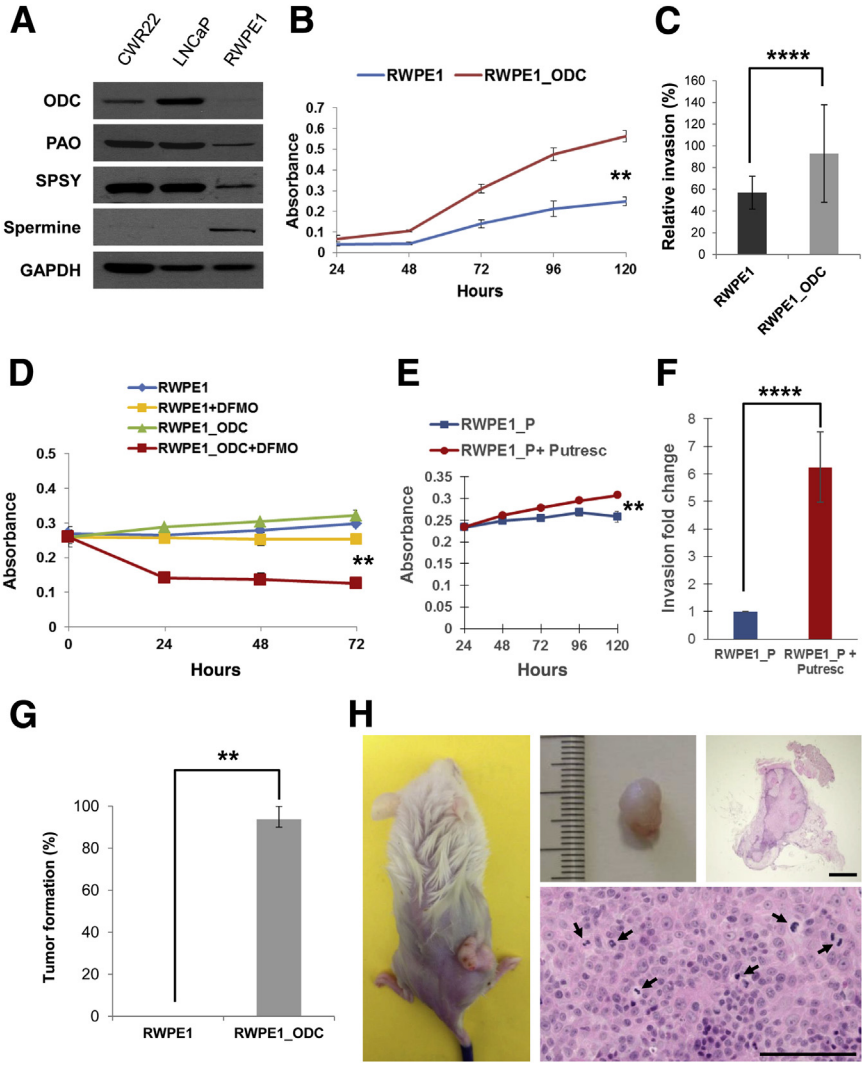

Figure 2 *ODC* is critical for malignant transformation in prostate cells. **A:** Representative immunoblot illustrating the expression of the main enzymes of the polyamine pathway and spermine abundance in the normal RWPE1 cell line, compared to the prostate cancer cell lines CWR22 and LnCaP. **B:** Quantification of proliferation by MTS assay at 24, 48, 72, 96, and 120 hours after seeding. Three independent experiments for each time point are represented (*t*-test). **C:** Quantification of three independent experiments of Matrigel invasion assay (*t*-test). **D:** Quantification of proliferation by MTS assay at 24, 48, and 72 hours after seeding and treating with D,L-α-difluoromethylornithine (DFMO). Three independent experiments for each time point are represented (*t*-test). **E:** Quantification of proliferation by MTS assay at 24, 48, 96, and 120 hours after seeding and treating with 100 μmol/L of putrescine. Three independent experiments for each time point are represented (*t*-test). **F:** Quantification of Matrigel invasion assay comparing RWPE1_P with regular medium or with putrescine treatment. Three independent experiments for each time point are represented (*t*-test). **G:** Tumor initiation experiments showed that RWPE1_ODC cells had a high de novo tumor initiation capacity (tumors formed in 45 of 48 injection sites for the RWPE1_ODC cells). Three independent experiments were performed (*t*-test). **H:** Gross and microscopic appearance of a representative tumor that formed after s.c. injection of 1×10^6 RWPE1_ODC cells in immunodeficient mice. **Arrows** point to mitotic figures observed in the tumor. $n = 6$ for each time point and cell line for experiment (**B**–**F**); $n = 16$ for each cell line (**G**). $^{**}P < 0.01$, $^{****}P < 0.0001$. Scale bars = 200 μm (**H**). GAPDH, glyceraldehyde-3-phosphate dehydrogenase; MTS, 3-(4,5-dimethylthiazol-2-yl)-5-(3-carboxymethoxyphenyl)-2-(4-sulfophenyl)-2H-tetrazolium; ODC, ornithine decarboxylase; PAO, polyamine oxidase; SPSY, spermine synthase.

genes in RWPE1_ODC cells (limma test, $P < 0.05$ and greater than twofold change) (Supplemental Figure S1A). The top 60 up-regulated and down-regulated genes between RWPE1 and RWPE1_ODC are listed in Table 3. As expected, the gene ontology analysis for biological processes showed that many metabolic processes were up-regulated in the cells with an activated polyamine pathway (Figure 3A). Some of the genes that were up-regulated, such as *MAPK* and *MMP13*, are associated with increased metabolism and invasion, whereas down-regulated genes included those associated with mitochondrial dysfunction and signaling pathways involved in malignant transformation, such as *EIF2* and *mTOR* (Supplemental Figure S1, B–D). These findings were confirmed at the protein level (Figure 3B). More specifically, p-mTOR and p-70S6kinase expression levels were lower in the RWPE1_ODC cells than in the parental cells. In contrast, p-MAP3K expression was slightly higher in the ODC-overexpressing cells, with protein levels similar to the CWR22 prostate cancer cells. Interestingly, both total mTOR and total MAP3K remained unchanged. Altogether, these results demonstrate, for the first time, that activation of the metabolic pathway is sufficient for prostate tumor initiation, and is linked to specific alterations involving signaling networks critical for maintenance of cellular homeostasis (Supplemental Figure S2A).[25]

ODC Gene Regulates *AR* Transcription Targets in Normal and Prostate Cancer Cells

To elucidate whether *ODC* regulates *AR* signaling in prostate cells, we analyzed a subset of *AR*-target genes (eg, *PSA*, *TMPRSS2*, *FKBP5*, and *ERG*) in RWPE1_P and RWPE1_ODC cells by RT-qPCR. These analyses revealed that these genes were significantly overexpressed in the RWPE1_ODC cells, only after Dihydrotestosterone treatment (Figure 3C). To further confirm this link, we transiently knocked down *ODC* in two *AR*-dependent prostate cancer cell lines (LNCaP and VCaP). These studies revealed that *AR*, as well as other well-known *AR*-target genes, was

Table 3 List of the Top 60 Genes of the 113 Up-Regulated and 234 Down-Regulated Genes between RWPE1 and RWPE1_ODC

Up-regulated genes			Down-regulated genes		
Gene name	*P* value	Fold change	Gene name	*P* value	Fold change
HCG2P7	0.043362	8.699880252	*APTX*	3.52×10^{-9}	−7.05842823
TXNL2	0.049122	7.829825014	*ITGB4*	0.046939	−6.66785551
AP3M1	0.039578	6.289572722	*C20ORF7*	0.049135	−6.01590958
TRAF3IP2	4.29×10^{-9}	6.10987277	*TMEM218*	0.037714	−5.00290573
MAP3K4	8.58×10^{-9}	5.673337574	*MFAP2*	0.040073	−4.87076243
ARFGAP3	2.24×10^{-8}	5.611857728	*TSC22D3*	0.000163	−4.70222855
OLFM4	0.041942	4.942136094	*ALAD*	0.029013	−4.5713245
C10ORF61	0.042706	4.795673117	*SLC25A25*	0.043912	−4.49495234
KIF18A	5.53×10^{-7}	4.119945152	*FBXL5*	1.07×10^{-5}	−4.49288692
KLK3	0.04459	3.973581652	*VEGFA*	0.048416	−4.07647083
BZW1	1.11×10^{-7}	3.878693704	*STEAP1*	0.042833	−3.8271634
CHKB	0.03817	3.807354922	*SLC6A10P*	9.55×10^{-8}	−3.6042244
C6ORF108	5.82×10^{-6}	3.804026904	*ARTN*	5.21×10^{-5}	−3.59655048
KRT19	9.32×10^{-7}	3.433820975	*RNF5*	0.049682	−3.56543994
HYAL2	0.022243	3.303191532	*MAP2K5*	0.035137	−3.56150353
FAIM	5.69×10^{-5}	3.230679033	*NCRNA00152*	0.028316	−3.48459554
TRAF6	0.045793	3.057030945	*STXBP1*	5.91×10^{-7}	−3.37223318
ENTPD3	2.08×10^{-7}	2.976541027	*DENND4A*	0.042738	−3.169925
HEY2	0.005789	2.878693704	*MFI2*	0.021025	−3.1490915
VAPA	0.029251	2.865982652	*KIAA1704*	0.029999	−3.11726605
SULT1E1	0.030167	2.827163403	*RPRML*	0.003449	−2.82059075
RTKN2	0.0059	2.800691192	*MARCH4*	0.014532	−2.63076619
NUPL1	2.27×10^{-5}	2.766902878	*MIR330*	0.002721	−2.52961947
ADAM23	8.15×10^{-5}	2.696855381	*HS.123511*	0.005457	−2.52153712
GPX7	0.019206	2.521537121	*IFNK*	0.021435	−2.4970148
PTGS2	0.00074	2.451893572	*NGF*	0.009074	−2.27517984
GREM1	6.12×10^{-5}	2.420843121	*SFTA1P*	0.006957	−2.24853484
AQP3	0.000148	2.31259023	*FAIM3*	0.018611	−2.1324503
MMP13	0.0009	2.277909628	*FAM25G*	0.031209	−2.12637729
ARMCX2	0.008776	1.974988112	*HS.553310*	0.005057	−2.12261929

significantly down-regulated at both the transcript and protein levels in the small interfering RNA technology against−ODC cells (Figure 3D). Furthermore, when we knocked down ODC in these prostate cancer cells, their proliferative activity diminished significantly (Figure 3E). These results confirm that *ODC* and *AR* are mutually regulated and may imply that overexpression of the ODC protein causes malignant transformation through activation of the AR axis, which, in turn, can affect different pathways involved in cell proliferation, cell survival, and tumor invasion.

The Polyamine Pathway Is Up-Regulated in Prostate Cancer, as Early as HGPIN

We followed the above-mentioned mechanistic studies with translational analyses aimed at deciphering the clinical significance of an increased metabolic pathway in prostate cancer (Supplemental Figure S2B). We performed immunophenotyping of the patients' tissues using specific antibodies to ODC, PAO, SPSY, and spermine. Patient characteristics are summarized in Table 2. Fifty-seven patients (54%) had no evidence of biochemical recurrence, with a median follow-up of 62.0 months (range, 3.0 to 187.0 months). Of the patients who showed biochemical relapse after surgery, 19 (40%) died of the disease. At the time of analysis, overall survival was 76%, with a median follow-up of 103.6 months (range, 3.0 to 222 months). The analysis of clinicopathological characteristics in relation to biochemical recurrence-free survival revealed, as expected, that surgical Gleason score ($P < 0.0001$) and preoperative PSA levels ($P = 0.034$) were significantly associated with a worse prognosis, thus validating the studied cohort. However, the pathologic stage of tumors did not significantly correlate with biochemical recurrence-free survival ($P = 0.400$) (Supplemental Figure S3).

The immunophenotyping analyses revealed that expression of the polyamine enzymes was low in the epithelial cells lining normal prostate glands, whereas epithelial cells in malignant glands, including both HGPIN and prostate cancer samples, showed intense cytoplasmic expression of ODC, PAO, and SPSY (Figure 4A). Notably, spermine abundance showed the opposite trend, being high in normal tissue and almost absent in tumor areas (Figure 4, A and B, and Table 4). After quantification, mean expression values of the three

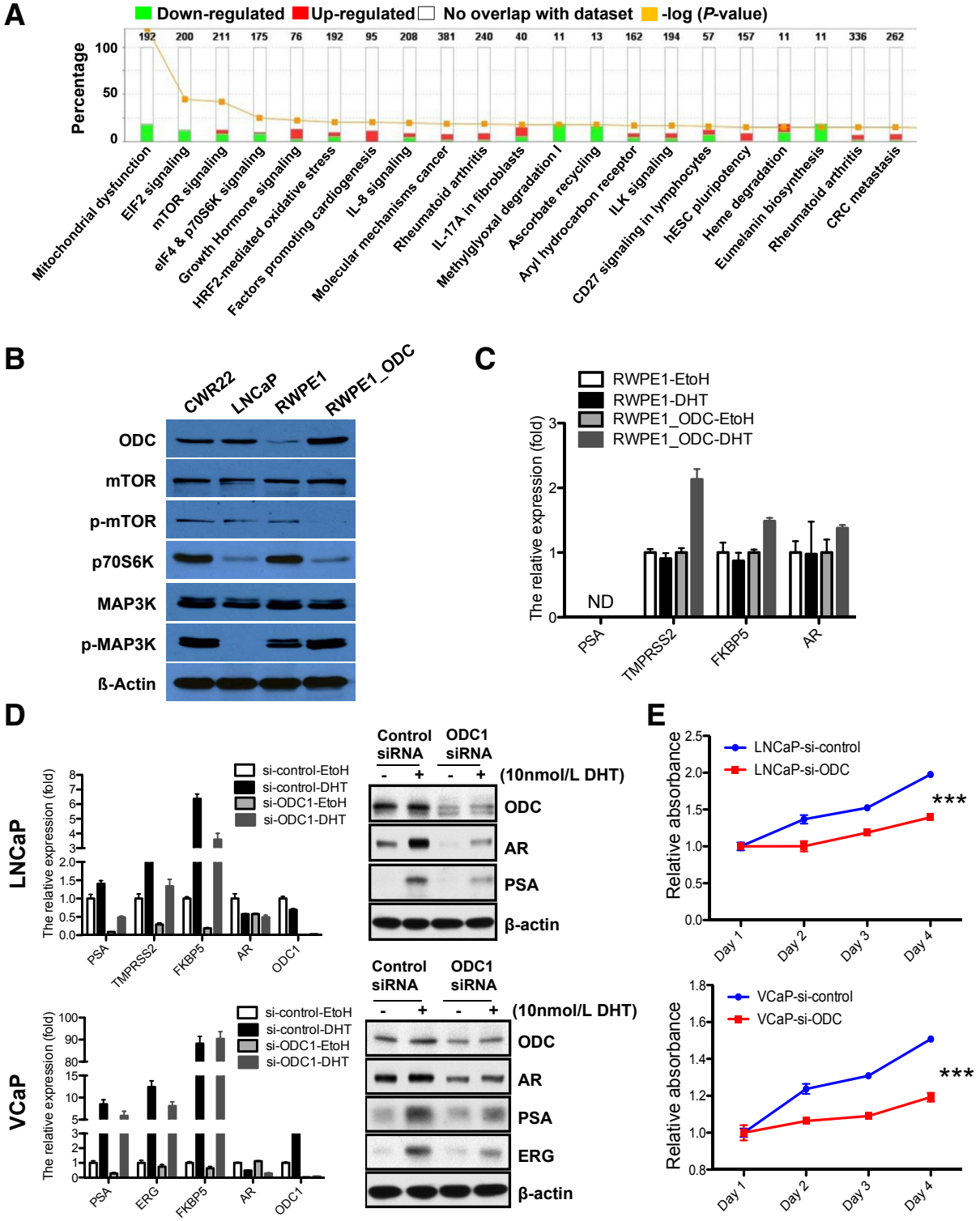

Figure 3 Polyamine pathway activation regulates critical genetic pathways as well as androgen receptor (AR) signaling. **A:** Gene ontology pathway analysis of the most frequent and significantly up-regulated and down-regulated genes in RWPE1_ODC cells. **B:** Representative immunoblot of the most critical proteins [mammalian target of rapamycin (mTOR), p70S6K, and mitogen-activated protein kinase (MAPK)] confirmed the alteration in several genetic pathways involved in cancer at the protein level. **C:** Quantification of the relative fold increase of well-known AR target mRNA gene levels in the RWPE1_ODC compared to the parental cells (*t*-test). **D:** Knocking down of ornithine decarboxylase (ODC) in LNCaP and VCaP cells significantly reduces mRNA and protein expression levels of AR and well-known AR target genes by RT-qPCR and immunoblot, respectively (*t*-test). **E:** Proliferation activity is reduced in prostate cancer cells after knocking down of ODC. Three independent experiments were performed (*t*-test). $n = 3$ for each cell line for experiment (**C** and **D**); $n = 6$ for each time point and cell line (**E**). ***$P < 0.001$. DHT, dihydrotestosterone; EtOH, ethanol; ERG, erythroblast transformation-specific–related gene; ND, not detected; PSA, prostate-specific antigen; si, small interfering RNA technology against.

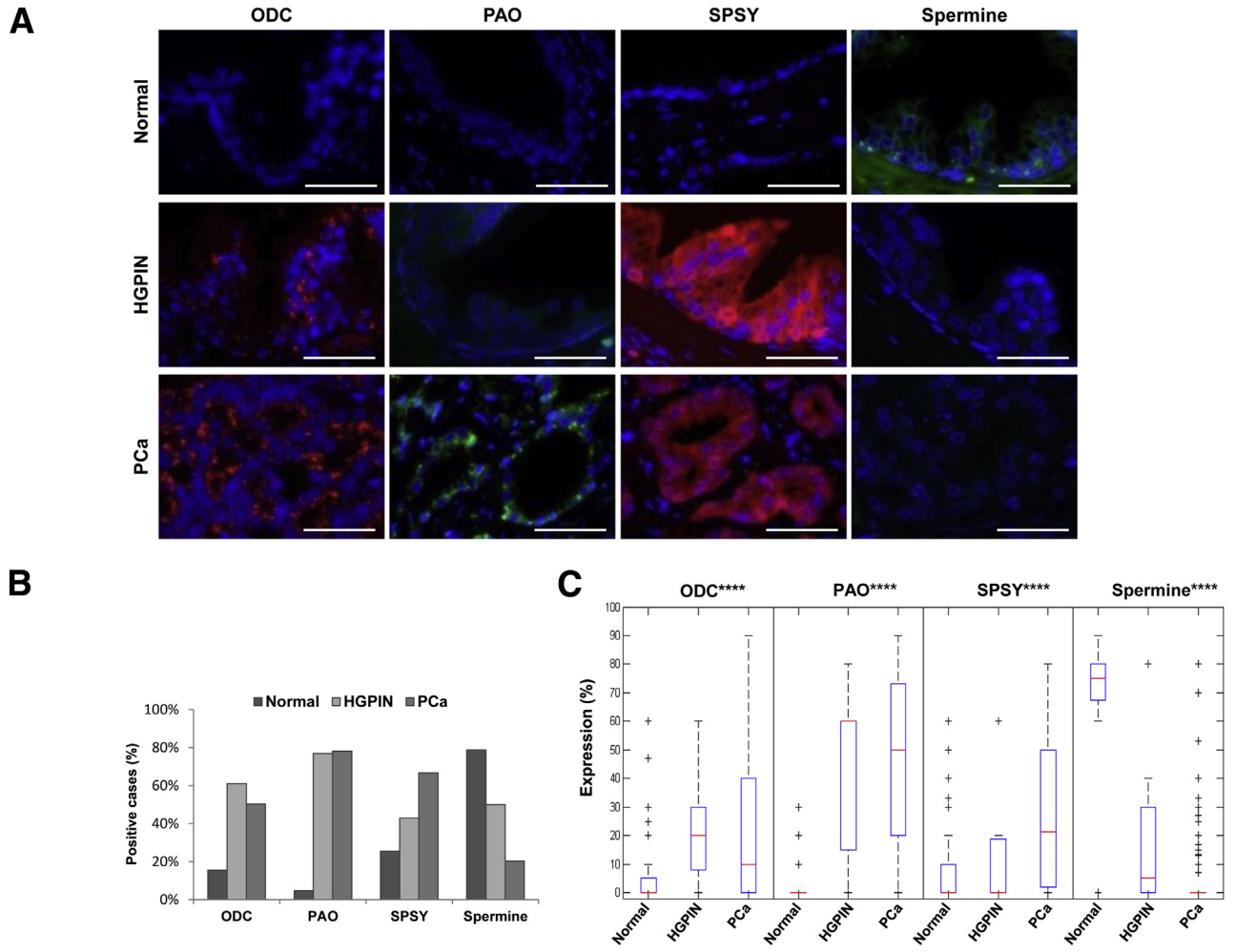

Figure 4 The polyamine pathway is activated in prostate cancer (PCa) and high-grade prostatic intraepithelial neoplasia (HGPIN) when compared to normal prostatic glands (Normal). **A:** Representative immunofluorescence analyses of PA pathway enzymes and spermine abundance in normal prostatic glands, HGPIN, and PCa. **B:** Bar diagram illustrates the percentage of samples with overexpression of PA pathway enzymes and down-regulation of spermine in normal prostate, HGPIN, and PCa (using a cutoff of 10%). **C:** Box-plot diagram illustrates expression levels of the main PA pathway enzymes and spermine abundance in normal prostate, HGPIN, and PCa. Data are expressed as means ± SD (analysis of variance test; **C**). ****$P < 0.0001$ (analyses of variances test between the three different groups). Scale bars = 100 μm (**A**). ODC, ornithine decarboxylase; PA, polyamine; PAO, polyamine oxidase; SPSY, spermine synthase.

enzymes in normal tissue corresponded to 6.7% ± 13.6% for ODC, 1.0% ± 5.1% for PAO, 7.4% ± 5.1% for SPSY, and 62.2% ± 33.3% for spermine abundance (Figure 4C). Notably, we observed that expression levels of the polyamine enzymes were significantly higher in HGPIN and prostate cancer samples than in normal prostate glands, which had significantly lower abundance of spermine ($P < 0.0001$) (Figure 4C).

All enzymes showed a direct and significant correlation among themselves (Table 5). For example, of the tumors that were characterized by an ODC-positive phenotype, 72.2% expressed PAO ($P < 0.0001$) and 63.4% expressed SPSY ($P < 0.001$). Similarly, 52.3% of tumors with a PAO-positive phenotype overexpressed ODC ($P < 0.0001$), and 47.3% of tumors with a SPSY-positive phenotype overexpressed ODC ($P < 0.001$). Furthermore, spermine abundance correlated inversely with the expression of all of the analyzed polyamine pathway enzymes: loss of spermine was observed in 68.8% ($P < 0.01$), 75.7% ($P < 0.0001$), and 70.7% ($P < 0.0001$) of the ODC-positive, PAO-positive, and SPSY-positive tumors, respectively (Table 5). Summarizing these results, we can conclude that there was a consistent pattern of expression in the polyamine pathway (specifically, an overexpression of the three enzymes and loss of spermine) that was characteristic of malignant transformation (Figure 5, A and B), similar to previous reports studying mRNA expression.[26–28] Notably, most of the analyzed HGPIN lesions showed the same immunophenotype as their adjacent prostate cancer lesions (Figure 5C), and only 12% of these HGPIN lesions were characterized by a different pattern, showing high abundance of spermine and lack of expression of ODC (Figure 5D).

Table 4 Samples with Overexpression of PA Pathway Enzymes and Down-Regulation of Spermine in Normal Prostate, HGPIN, and PCa (Using a Cutoff of 10%)

Variable	Normal	HGPIN	PCa
ODC****	15.5	61.1	50.4
PAO****	4.7	76.9	78.2
SPSY****	25.5	42.9	66.7
Spermine****	78.8	50.0	20.3

Data are given as percentage.

****$P < 0.0001$.

HGPIN, high-grade prostate intraepithelial neoplasia; ODC, ornithine decarboxylase; PA, polyamine; PAO, polyamine oxidase; PCa, prostate cancer; SPSY, spermine synthase.

Polyamine Pathway Immunophenotypes and Their Association with Clinicopathological Variables and Patient Outcome

When we examined the associations between the analyzed polyamine pathway enzymes/amine and the main clinicopathological variables (Supplemental Table S1), we observed that only the ODC-positive phenotype correlated significantly with Gleason score ($P < 0.05$) and pathological stage ($P < 0.01$), whereas the other enzymes and spermine abundance did not. Furthermore, we did not observe any association between polyamine pathway enzymes/amine and biochemical recurrence-free survival (Supplemental Figure S4A) or overall survival (Supplemental Figure S4B).

Discussion

The metabolic polyamine pathway has been previously reported to be critical for the maintenance of homeostatic processes, such as cell growth, apoptosis, mitochondrial function, autophagy, and gene regulation (Supplemental Figure S2A).[25] More specifically, *ODC*, the gene coding for the rate-limiting enzyme of this pathway, has been reported to be a target gene in the pleiotropic androgen-responsive biology of prostate cancer.[7,28] This relationship is also observed in skeletal muscle, where *ODC* is up-regulated by the androgen receptor, promoting cell proliferation and delayed differentiation, both of which are features of tumor formation.[29] Even though some authors have reported how polyamine pathway controls cell cycle,[30] *ODC* functional contribution in prostate tumor initiation has not been fully explored to date.

Table 5 PCa Cases with Specific Phenotypes Displayed

Variable	ODC^+	PAO^+	$SPSY^+$	$Spermine^-$
ODC^+	NA	72.2****	63.4***	68.8**
PAO^+	52.3****	NA	66.0****	75.7****
$SPSY^+$	47.3***	64.8****	NA	70.7****
$Spermine^-$	44.5**	67.8****	59.8****	NA

Data are given as percentage.

**$P < 0.01$, ***$P < 0.001$, and ****$P < 0.0001$.

NA, not applicable; ODC, ornithine decarboxylase; PAO, polyamine oxidase; PCa, prostate cancer; SPSY, spermine synthase.

Others have previously demonstrated the transformation capacity of ODC overexpression in fibroblasts[1,31,32]; nonetheless, this is the first study, to our knowledge, to functionally implicate ODC as a critical and sufficient enzyme in the malignant transformation of prostatic epithelium both *in vitro* and *in vivo*. Some earlier studies described that polyamine pathway gene expression signatures were linked to prostate cancer,[26,27] but only a few reports with small cohorts of patients have described the increase of ODC protein expression in prostate cancer as compared to normal prostate tissue.[6,16,33] In our series of 120 well-characterized prostate cancer patients, we found ODC overexpression in 61% of the 18 HGPIN lesions and 50% of invasive prostate cancer samples analyzed. This suggests that the polyamine pathway enzymes could be involved in the early stages of carcinogenesis and could promote the progression from HGPIN to invasive carcinoma. Previously, preclinical imaging studies with positron emission tomography have explored the potential roles of different radiolabeled polyamines as prostate imaging agents.[34,35] Herein, we show, for the first time, that overexpression of ODC in a normal prostate cell line confers de novo tumor initiation capacity. Functionally, in comparison to its parental cell line, the new ODC-overexpressing cell line showed higher proliferation activity and higher invasion potential through the activation of signaling pathways commonly associated with cancer. Gene expression analysis comparing parental RWPE1 and RWPE1_ODC cells revealed that specific transcription factors and signaling pathways, including *MAPK*, *CHKB*, *MMP13*, mitochondrial dysfunction, *EIF2*, and *mTOR*, were altered in the RWPE1_ODC cells, and these findings were confirmed at the protein level.

These results demonstrate that prostate tumorigenesis may be promoted by the activation of the polyamine pathway through the above-mentioned cancer-related genes. Our findings in the ODC-overexpressing cells were consistent with literature showing that *MAPK* and *CHKB* were up-regulated in prostate cancer. The *RAS/MAPK* pathway is significantly elevated in both primary and metastatic prostate cancer, and its activation promotes aggressive tumor behavior, but there is no information about its implication in tumor initiation.[36,37] Although *CHKB* has been shown to be involved in carcinogenesis in different types of solid tumors, to our knowledge, it has not been studied in human prostate cancer.[38] Different metalloproteinases, including *MMP13*, which has previously been linked to prostate cancer, were also up-regulated in the ODC-overexpressing cells in our study.[39] Mitochondrial dysfunction and *EIF2* and *mTOR* signaling pathways were found to be the most significantly altered genetic pathways in conjunction with the polyamine pathway's increased activity. Defects in mitochondrial function, which are important in cellular metabolism and apoptosis, have long been known to contribute to the development and progression of cancer.[40] Similarly, *EIF2*

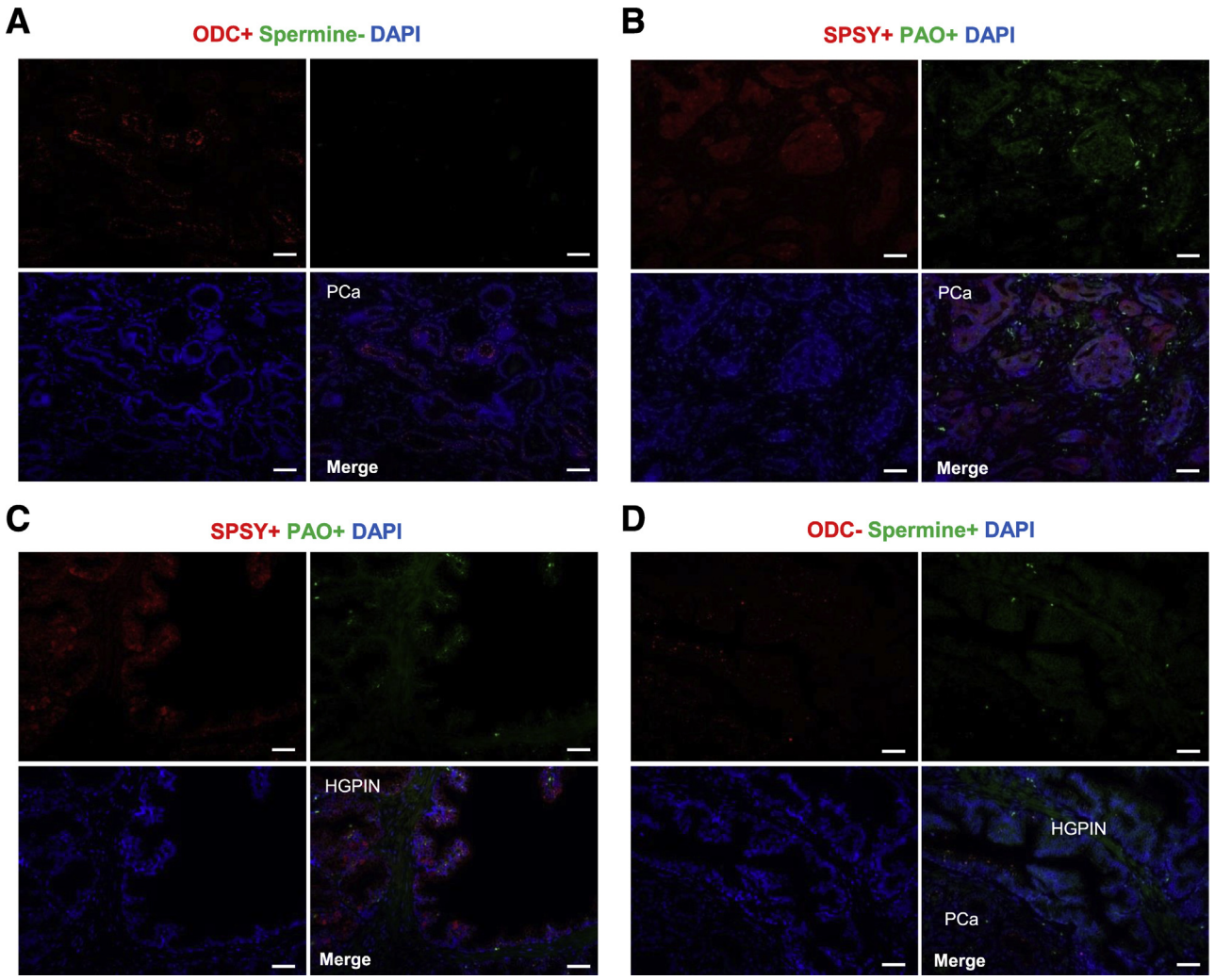

Figure 5 Prostate cancer is characterized by direct correlation between the expression of polyamine pathway enzymes and inverse correlation of these enzymes with spermine abundance. **A**–**D:** Representative immunofluorescence analysis of PA pathway enzymes' expression and spermine abundance in prostate cancer (PCa) and high-grade prostatic intraepithelial neoplasia [HGPIN; ornithine decarboxylase (ODC) and spermine in **A** and **D**; polyamine oxidase (PAO) and spermine synthase (SPSY) in **B** and **C**]. Scale bars = 100 μm (**A**–**D**). PA, polyamine.

has been associated with hypoxia and metabolism in cancer cells, making it one of the most critical pathways involved in malignant transformation.[41] The *mTOR* pathway has been extensively studied in prostate cancer and tumorigenesis.[42,43] Inhibition of *mTORC1* has been shown to lead to *MAPK* pathway activation, which is consistent with the results we observed after polyamine pathway activation.[44]

Several gene alterations, such as decreased *GSTP1* and *Nkx3.1* expression, have been implicated in the malignant transformation of normal prostate epithelium to HGPIN.[45] HGPIN is a precursor of invasive prostate carcinoma,[46,47] but little is known about the genetic events involved in the advancement to invasive disease,[48,49] a sequence of events that remains unclear.[50] Few studies have shown specific genetic alterations in HGPIN, including in the *SIRT1/S6K* axis, *mTOR-RAPTOR* pathway, *PEDF*, and miR-21,[51–54] but much remains unexplained. In the present study, we show that the polyamine pathway plays a unique role in early prostate transformation, being already altered in HGPIN lesions; therefore, ODC, PAO, SPSY, and spermine could play an important role in improving early detection and risk stratification of prostate cancer.

A single study has validated tissue-based expression levels of spermine in prostate cancer by immunohistochemistry.[8] In our study, spermine was abundant in normal prostatic glands (mean, 62.2%) and lost during malignant transformation, as early as HGPIN (mean, 18.8% in HGPIN and 5.8% in prostate cancer). Our results show that ODC, PAO, and SPSY levels are commonly up-regulated in HGPIN tissues as compared to normal prostate glands, with the expression levels for PAO expression being the highest of the three (mean, 5.1% in normal prostate tissue versus 41.2% in HGPIN). Notably, expression of these polyamine pathway enzymes in prostate cancer was similar to the expression of the same enzymes in HGPIN (eg, mean PAO

level was 46.0% in prostate cancer), which further highlights the importance of these markers in prostate tumorigenesis. In a smaller patient cohort, Goodwin et al[5] found that PAO was up-regulated in HGPIN and prostate cancer as compared to benign prostate tissue.

It is well known that the polyamine pathway can be successfully inhibited by specific enzyme inhibitors, such as DFMO for ODC. We showed that treatment of RWPE1-ODC cells with DFMO reduced the proliferation activity to levels similar to those seen in RWPE1 parental cells. Although a phase 2 clinical trial of DFMO with patients with a family history of prostate cancer but no previous personal history of prostate cancer has been reported,[55] no trials have included patients with a diagnosis of HGPIN and no evidence of prostate cancer. Different chemopreventive clinical trials have been developed to control progression of HGPIN to prostate cancer using selenium, soy, vitamin E,[56,57] toremifene,[58] or green tea extract,[59,60] with different success rates. Our findings suggest that DFMO treatment, which is usually associated with minimal toxicity,[61] may prove valuable for reducing the development of prostate cancer in patients with a diagnosis of HGPIN and may play a crucial role in future chemopreventive clinical trials.

Acknowledgments

We thank Dr. Rong Wang and Dr. Georgia Dolios (Mass Spectrometry, Proteomics and Metabolomics Core Facility at the Icahn Institute) for performing the spermine mass spectrometry analyses in cell culture media and cell pellets (data not shown). These extra studies were performed to confirm the presence of spermine in cell extracts and media, as per Reviewers' comment. We also thank Sandhya George and Ada Muellner for editing the manuscript.

A.S.-D. designed the study and wrote the manuscript; M.C.-M. designed the study, developed the method, performed and supervised several of the *in vitro* and *in vivo* experiments, performed the analyses, and wrote the manuscript; M.C. performed all of the siRNA *in vitro* experiments; J.L. performed the overexpression and several of the *in vitro* experiments; N.G. performed several of the *in vitro* experiments and reviewed the manuscript; A.C.L. performed several of the *in vitro* and *in vivo* experiments and reviewed the manuscript; F.M.K. performed the sample size calculation and most of the statistical analyses; V.P. supervised the overexpression experiments; Z.Y. and W.Z. performed all of the gene expression analyses, provided the diagrams to illustrate the results, and uploaded the data in the Gene Expression Omnibus repository website; P.P.P. supervised the performance of several experiments and reviewed the manuscript; H.H. supervised the writing of the manuscript; and C.C.-C. designed the study, supervised all of the experiments, and wrote the manuscript.

C.C.-C. is the guarantor of this work and, as such, had full access to all of the data in the study and takes responsibility for the integrity of the data and the accuracy of the data analysis.

Supplemental Data

Supplemental material for this article can be found at *http://dx.doi.org/10.1016/j.ajpath.2016.08.021*.

References

1. Auvinen M, Paasinen A, Andersson LC, Holtta E: Ornithine decarboxylase activity is critical for cell transformation. Nature 1992, 360: 355–358
2. Cipolla B, Guille F, Moulinoux JP, Quemener V, Staerman F, Corbel L, Lobel B: Polyamines and prostatic carcinoma: clinical and therapeutic implications. Eur Urol 1993, 24:124–131
3. Gerner EW, Meyskens FL Jr: Polyamines and cancer: old molecules, new understanding. Nat Rev Cancer 2004, 4:781–792
4. Nowotarski SL, Woster PM, Casero RA Jr: Polyamines and cancer: implications for chemotherapy and chemoprevention. Expert Rev Mol Med 2013, 15:e3
5. Goodwin AC, Jadallah S, Toubaji A, Lecksell K, Hicks JL, Kowalski J, Bova GS, De Marzo AM, Netto GJ, Casero RA Jr: Increased spermine oxidase expression in human prostate cancer and prostatic intraepithelial neoplasia tissues. Prostate 2008, 68: 766–772
6. Young L, Salomon R, Au W, Allan C, Russell P, Dong Q: Ornithine decarboxylase (ODC) expression pattern in human prostate tissues and ODC transgenic mice. J Histochem Cytochem 2006, 54:223–229
7. Bai G, Kasper S, Matusik RJ, Rennie PS, Moshier JA, Krongrad A: Androgen regulation of the human ornithine decarboxylase promoter in prostate cancer cells. J Androl 1998, 19:127–135
8. Cohen RJ, Fujiwara K, Holland JW, McNeal JE: Polyamines in prostatic epithelial cells and adenocarcinoma: the effects of androgen blockade. Prostate 2001, 49:278–284
9. Jung JA, Coakley FV, Vigneron DB, Swanson MG, Qayyum A, Weinberg V, Jones KD, Carroll PR, Kurhanewicz J: Prostate depiction at endorectal MR spectroscopic imaging: investigation of a standardized evaluation system. Radiology 2004, 233:701–708
10. Kurhanewicz J, Vigneron DB, Hricak H, Narayan P, Carroll P, Nelson SJ: Three-dimensional H-1 MR spectroscopic imaging of the in situ human prostate with high (0.24-0.7-cm^3) spatial resolution. Radiology 1996, 198:795–805
11. Shukla-Dave A, Hricak H, Moskowitz C, Ishill N, Akin O, Kuroiwa K, Spector J, Kumar M, Reuter VE, Koutcher JA, Zakian KL: Detection of prostate cancer with MR spectroscopic imaging: an expanded paradigm incorporating polyamines. Radiology 2007, 245:499–506
12. van der Graaf M, Schipper RG, Oosterhof GO, Schalken JA, Verhofstad AA, Heerschap A: Proton MR spectroscopy of prostatic tissue focused on the detection of spermine, a possible biomarker of malignant behavior in prostate cancer. MAGMA 2000, 10:153–159
13. Konishi N, Shimada K, Ishida E, Nakamura M: Molecular pathology of prostate cancer. Pathol Int 2005, 55:531–539
14. Abate-Shen C, Shen MM: Molecular genetics of prostate cancer. Genes Dev 2000, 14:2410–2434
15. Di Cristofano A, De Acetis M, Koff A, Cordon-Cardo C, Pandolfi PP: Pten and p27KIP1 cooperate in prostate cancer tumor suppression in the mouse. Nat Genet 2001, 27:222–224
16. Tomlins SA, Mehra R, Rhodes DR, Cao X, Wang L, Dhanasekaran SM, Kalyana-Sundaram S, Wei JT, Rubin MA, Pienta KJ, Shah RB, Chinnaiyan AM: Integrative molecular concept modeling of prostate cancer progression. Nat Genet 2007, 39:41–51

17. Tomlins SA, Rhodes DR, Perner S, Dhanasekaran SM, Mehra R, Sun XW, Varambally S, Cao X, Tchinda J, Kuefer R, Lee C, Montie JE, Shah RB, Pienta KJ, Rubin MA, Chinnaiyan AM: Recurrent fusion of TMPRSS2 and ETS transcription factor genes in prostate cancer. Science 2005, 310:644–648
18. Mosquera JM, Perner S, Genega EM, Sanda M, Hofer MD, Mertz KD, Paris PL, Simko J, Bismar TA, Ayala G, Shah RB, Loda M, Rubin MA: Characterization of TMPRSS2-ERG fusion high-grade prostatic intraepithelial neoplasia and potential clinical implications. Clin Cancer Res 2008, 14:3380–3385
19. Jung SH, Shin S, Kim MS, Baek IP, Lee JY, Lee SH, Kim TM, Lee SH, Chung YJ: Genetic progression of high grade prostatic intraepithelial neoplasia to prostate cancer. Eur Urol 2016, 69: 823–830
20. Bello D, Webber MM, Kleinman HK, Wartinger DD, Rhim JS: Androgen responsive adult human prostatic epithelial cell lines immortalized by human papillomavirus 18. Carcinogenesis 1997, 18: 1215–1223
21. Likar Y, Zurita J, Dobrenkov K, Shenker L, Cai S, Neschadim A, Medin JA, Sadelain M, Hricak H, Ponomarev V: A new pyrimidine-specific reporter gene: a mutated human deoxycytidine kinase suitable for PET during treatment with acycloguanosine-based cytotoxic drugs. J Nucl Med 2010, 51:1395–1403
22. Saeed AI, Sharov V, White J, Li J, Liang W, Bhagabati N, Braisted J, Klapa M, Currier T, Thiagarajan M, Sturn A, Snuffin M, Rezantsev A, Popov D, Ryltsov A, Kostukovich E, Borisovsky I, Liu Z, Vinsavich A, Trush V, Quackenbush J: TM4: a free, open-source system for microarray data management and analysis. Biotechniques 2003, 34:374–378
23. Tsai YH, Lin KL, Huang YP, Hsu YC, Chen CH, Chen Y, Sie MH, Wang GJ, Lee MJ: Suppression of ornithine decarboxylase promotes osteogenic differentiation of human bone marrow-derived mesenchymal stem cells. FEBS Lett 2015, 589:2058–2065
24. Farriol M, Segovia-Silvestre T, Castellanos JM, Venereo Y, Orta X: Role of putrescine in cell proliferation in a colon carcinoma cell line. Nutrition 2001, 17:934–938
25. Minois N, Carmona-Gutierrez D, Madeo F: Polyamines in aging and disease. Aging (Albany NY) 2011, 3:716–732
26. Bettuzzi S, Davalli P, Astancolle S, Carani C, Madeo B, Tampieri A, Corti A: Tumor progression is accompanied by significant changes in the levels of expression of polyamine metabolism regulatory genes and clusterin (sulfated glycoprotein 2) in human prostate cancer specimens. Cancer Res 2000, 60:28–34
27. Bettuzzi S, Scaltriti M, Caporali A, Brausi M, D'Arca D, Astancolle S, Davalli P, Corti A: Successful prediction of prostate cancer recurrence by gene profiling in combination with clinical data: a 5-year follow-up study. Cancer Res 2003, 63:3469–3472
28. Betts AM, Waite I, Neal DE, Robson CN: Androgen regulation of ornithine decarboxylase in human prostatic cells identified using differential display. FEBS Lett 1997, 405:328–332
29. Lee NK, Skinner JP, Zajac JD, MacLean HE: Ornithine decarboxylase is upregulated by the androgen receptor in skeletal muscle and regulates myoblast proliferation. Am J Physiol Endocrinol Metab 2011, 301:E172–E179
30. Bettuzzi S, Davalli P, Astancolle S, Pinna C, Roncaglia R, Boraldi F, Tiozzo R, Sharrard M, Corti A: Coordinate changes of polyamine metabolism regulatory proteins during the cell cycle of normal human dermal fibroblasts. FEBS Lett 1999, 446:18–22
31. Auvinen M, Laine A, Paasinen-Sohns A, Kangas A, Kangas L, Saksela O, Andersson LC, Holtta E: Human ornithine decarboxylase-overproducing NIH3T3 cells induce rapidly growing, highly vascularized tumors in nude mice. Cancer Res 1997, 57:3016–3025
32. Moshier JA, Dosescu J, Skunca M, Luk GD: Transformation of NIH/3T3 cells by ornithine decarboxylase overexpression. Cancer Res 1993, 53:2618–2622
33. Mohan RR, Challa A, Gupta S, Bostwick DG, Ahmad N, Agarwal R, Marengo SR, Amini SB, Paras F, MacLennan GT, Resnick MI, Mukhtar H: Overexpression of ornithine decarboxylase in prostate cancer and prostatic fluid in humans. Clin Cancer Res 1999, 5: 143–147
34. Palakurthi S, McQuarrie SA, Suresh MR: Screening of 14C-polyamines in the AT3B-1 rat prostate tumor model: the search for a new PET prostate imaging agent. In Vivo 2007, 21:823–828
35. Hwang DR, Lang LX, Mathias CJ, Kadmon D, Welch MJ: N-3-[18F]fluoropropylputrescine as potential PET imaging agent for prostate and prostate derived tumors. J Nucl Med 1989, 30: 1205–1210
36. Mukherjee R, McGuinness DH, McCall P, Underwood MA, Seywright M, Orange C, Edwards J: Upregulation of MAPK pathway is associated with survival in castrate-resistant prostate cancer. Br J Cancer 2011, 104:1920–1928
37. Mulholland DJ, Kobayashi N, Ruscetti M, Zhi A, Tran LM, Huang J, Gleave M, Wu H: Pten loss and RAS/MAPK activation cooperate to promote EMT and metastasis initiated from prostate cancer stem/-progenitor cells. Cancer Res 2012, 72:1878–1889
38. Gallego-Ortega D, Gomez del Pulgar T, Valdes-Mora F, Cebrian A, Lacal JC: Involvement of human choline kinase alpha and beta in carcinogenesis: a different role in lipid metabolism and biological functions. Adv Enzyme Regul 2011, 51:183–194
39. Morgia G, Falsaperla M, Malaponte G, Madonia M, Indelicato M, Travali S, Mazzarino MC: Matrix metalloproteinases as diagnostic (MMP-13) and prognostic (MMP-2, MMP-9) markers of prostate cancer. Urol Res 2005, 33:44–50
40. Carew JS, Huang P: Mitochondrial defects in cancer. Mol Cancer 2002, 1:9
41. Zhu K, Chan W, Heymach J, Wilkinson M, McConkey DJ: Control of HIF-1alpha expression by eIF2 alpha phosphorylation-mediated translational repression. Cancer Res 2009, 69:1836–1843
42. Nardella C, Carracedo A, Alimonti A, Hobbs RM, Clohessy JG, Chen Z, Egia A, Fornari A, Fiorentino M, Loda M, Kozma SC, Thomas G, Cordon-Cardo C, Pandolfi PP: Differential requirement of mTOR in postmitotic tissues and tumorigenesis. Sci Signal 2009, 2: ra2
43. Nardella C, Chen Z, Salmena L, Carracedo A, Alimonti A, Egia A, Carver B, Gerald W, Cordon-Cardo C, Pandolfi PP: Aberrant Rheb-mediated mTORC1 activation and Pten haploinsufficiency are cooperative oncogenic events. Genes Dev 2008, 22:2172–2177
44. Carracedo A, Ma L, Teruya-Feldstein J, Rojo F, Salmena L, Alimonti A, Egia A, Sasaki AT, Thomas G, Kozma SC, Papa A, Nardella C, Cantley LC, Baselga J, Pandolfi PP: Inhibition of mTORC1 leads to MAPK pathway activation through a PI3K-dependent feedback loop in human cancer. J Clin Invest 2008, 118: 3065–3074
45. Knudsen BS, Vasioukhin V: Mechanisms of prostate cancer initiation and progression. Adv Cancer Res 2010, 109:1–50
46. Clouston D, Bolton D: In situ and intraductal epithelial proliferations of prostate: definitions and treatment implications: part 2: intraductal carcinoma and ductal adenocarcinoma of prostate. BJU Int 2012, 110(Suppl 4):22–24
47. Montironi R, Mazzucchelli R, Lopez-Beltran A, Cheng L, Scarpelli M: Mechanisms of disease: high-grade prostatic intraepithelial neoplasia and other proposed preneoplastic lesions in the prostate. Nat Clin Pract Urol 2007, 4:321–332
48. Bostwick DG, Pacelli A, Lopez-Beltran A: Molecular biology of prostatic intraepithelial neoplasia. Prostate 1996, 29:117–134
49. Haggman MJ, Macoska JA, Wojno KJ, Oesterling JE: The relationship between prostatic intraepithelial neoplasia and prostate cancer: critical issues. J Urol 1997, 158:12–22
50. DeMarzo AM, Nelson WG, Isaacs WB, Epstein JI: Pathological and molecular aspects of prostate cancer. Lancet 2003, 361:955–964
51. Leite KR, Tomiyama A, Reis ST, Sousa-Canavez JM, Sanudo A, Camara-Lopes LH, Srougi M: MicroRNA expression profiles in the progression of prostate cancer-from high-grade prostate intraepithelial neoplasia to metastasis. Urol Oncol 2013, 31:796–801

52. Li G, Rivas P, Bedolla R, Thapa D, Reddick RL, Ghosh R, Kumar AP: Dietary resveratrol prevents development of high-grade prostatic intraepithelial neoplastic lesions: involvement of SIRT1/S6K axis. Cancer Prev Res (Phila) 2013, 6:27−39
53. Evren S, Dermen A, Lockwood G, Fleshner N, Sweet J: mTOR-RAPTOR and 14-3-3sigma immunohistochemical expression in high grade prostatic intraepithelial neoplasia and prostatic adenocarcinomas: a tissue microarray study. J Clin Pathol 2011, 64:683−688
54. Qingyi Z, Lin Y, Junhong W, Jian S, Weizhou H, Long M, Zeyu S, Xiaojian G: Unfavorable prognostic value of human PEDF decreased in high-grade prostatic intraepithelial neoplasia: a differential proteomics approach. Cancer Invest 2009, 27:794−801
55. Simoneau AR, Gerner EW, Nagle R, Ziogas A, Fujikawa-Brooks S, Yerushalmi H, Ahlering TE, Lieberman R, McLaren CE, Anton-Culver H, Meyskens FL Jr: The effect of difluoromethylornithine on decreasing prostate size and polyamines in men: results of a year-long phase IIb randomized placebo-controlled chemoprevention trial. Cancer Epidemiol Biomarkers Prev 2008, 17:292−299
56. Fleshner NE, Kapusta L, Donnelly B, Tanguay S, Chin J, Hersey K, Farley A, Jansz K, Siemens DR, Trpkov K, Lacombe L, Gleave M, Tu D, Parulekar WR: Progression from high-grade prostatic intraepithelial neoplasia to cancer: a randomized trial of combination vitamin-E, soy, and selenium. J Clin Oncol 2011, 29:2386−2390
57. Marshall JR, Tangen CM, Sakr WA, Wood DP Jr, Berry DL, Klein EA, Lippman SM, Parnes HL, Alberts DS, Jarrard DF, Lee WR, Gaziano JM, Crawford ED, Ely B, Ray M, Davis W, Minasian LM, Thompson IM Jr: Phase III trial of selenium to prevent prostate cancer in men with high-grade prostatic intraepithelial neoplasia: SWOG S9917. Cancer Prev Res (Phila) 2011, 4:1761−1769
58. Taneja SS, Morton R, Barnette G, Sieber P, Hancock ML, Steiner M: Prostate cancer diagnosis among men with isolated high-grade intraepithelial neoplasia enrolled onto a 3-year prospective phase III clinical trial of oral toremifene. J Clin Oncol 2013, 31:523−529
59. Bettuzzi S, Brausi M, Rizzi F, Castagnetti G, Peracchia G, Corti A: Chemoprevention of human prostate cancer by oral administration of green tea catechins in volunteers with high-grade prostate intraepithelial neoplasia: a preliminary report from a one-year proof-of-principle study. Cancer Res 2006, 66:1234−1240
60. Brausi M, Rizzi F, Bettuzzi S: Chemoprevention of human prostate cancer by green tea catechins: two years later: a follow-up update. Eur Urol 2008, 54:472−473
61. Zell JA, Pelot D, Chen WP, McLaren CE, Gerner EW, Meyskens FL: Risk of cardiovascular events in a randomized placebo-controlled, double-blind trial of difluoromethylornithine plus sulindac for the prevention of sporadic colorectal adenomas. Cancer Prev Res (Phila) 2009, 2:209−212